EPJ Web of Conferences **36**, 00004 (2012)
DOI: 10.1051/epjconf/20123600004


# Resonances from PHSD

E. L. Bratkovskaya[1,2,a]

[1] Institute for Theoretical Physics, University of Frankfurt, Frankfurt, Germany
[2] Frankfurt Institute for Advanced Studies, 60438 Frankfurt am Main

**Abstract.** The multi-strange baryon and vector meson resonance production in relativistic nucleus-nucleus collisions is studied within the parton-hadron-string dynamics (PHSD) approach which incorporates explicit partonic degrees-of-freedom in terms of strongly interacting quasiparticles (quarks and gluons) in line with an equation-of-state from lattice QCD as well as the dynamical hadronization and hadronic collision dynamics in the final reaction phase. We find a significant effect of the partonic phase on the production of multi-strange antibaryons at SPS energies due to a slightly enhanced $s\bar{s}$ pair production from massive time-like gluon decay and a larger formation of antibaryons in the hadronization process. We, futhermore, obtain a visible in-medium effects in the low mass dilepton sector from dynamical vector-meson spectral functions from SIS to SPS energies whereas at RHIC and LHC energies such medium effects become more moderate. In the intermediate mass regime from 1.1 to 3 GeV pronounced traces of the partonic degrees of freedom are found at SPS energies which superseed the hadronic (multi-meson) channels as well as the correlated and uncorrelated semi-leptonic $D$-meson decays. The dilepton production from the strongly interacting quark-gluon-plasma (sQGP) becomes already visible at top SPS energies and more pronounced at RHIC and LHC energies.

## 1 Introduction

The study of resonance production in heavy-ion collisions is considered as one of the promising ways to obtain information about the different reaction stages [1]. The resonances can be produced through out the whole history of the reaction at the hadronization of Quark-Gluon Plasma (QGP) as well as in hadronic phase by rescattring. Thus they can provide information about the partonic phase as well as about in-medium effects related to hadronic interactions. The resonances can decay to hadrons and some of them, as vector mesons, to leptonic modes. The hadronic decay mode is dominant whereas the leptonic decay (i.e. the production of dileptons - correlated electron-positron or $\mu^+\mu^-$ pairs) is a very rare process due to the small branching ratio. However, there is a big disadvantage to use the hadronic mode in order to expand in-medium properties of the hadrons: it is very difficult experimentally to identify the products of hadronic decays due to their strong interactions with the environments. In this respect the leptonic mode is more promising since dileptons interact only electromagnetically, i.e. very weakly with the strongly interacting partonic or hadronic medium created in the collisions. Thus dileptons can provide an undistorted information about the different phases of the reactions as well as about in-medium properties of resonances.

An important dilepton observable is the invariant mass spectrum which can be roughly divided in 3 different regions, in each of which different physics dominates the radiation. In the low mass region ($M_{e^+e^-} < 1$ GeV) the radiation is dominated by the decays of light

[a] e-mail: Elena.Bratkovskaya@th.physik.uni-frankfurt.de

mesons (consisting of $u$, $d$ and $s$ (anti)quarks) and especially gives information about in-medium properties of the $\rho^0$ meson. In the intermediate mass region (1.1 GeV $< M_{e^+e^-} <$ 3 GeV) the dominant contribution to the invariant mass spectrum is obtained from the decays of open charm mesons, while above the $J/\psi$ peak, first open beauty decays and later on initial state Drell-Yan radiation are expected to dominate the dilepton spectrum. On top of the previously mentioned sources, especially in the intermediate mass region, also radiation from the strongly interacting Quark-Gluon-Plasma (sQGP) can give a significant signal [2] as well as some other more exotic sources like simultaneous interactions of four pions [3–6]. These partonic and hadronic channels have been studied in detail in Refs. [7,8] at the top Super-Proton-Synchrotron (SPS) and Relativistic-Heavy-Ion-Collider (RHIC) energies and it has been found that the partonic channels clearly dominate over multi-pion sources in the intermediate dilepton mass regime.

This contribution aims to summarize the perspectives of dilepton measurements for studying the vector meson resonances produced in heavy-ion collisions at relativistic energies as well as to discuss the possible QGP effects on hadronic observables. As an example we consider the enhancement of (multi-) strange (anti-) baryons. Our study is based on the Parton-Hadron-String Dynamics (PHSD) transport model [9].

## 2 The PHSD approach

The dynamics of partons, hadrons and strings in relativistic nucleus-nucleus collisions is analyzed here within the Parton-Hadron-String Dynamics approach [9]. In this transport approach the partonic dynamics is based on Kadanoff-Baym equations for Green functions with self-energies from the Dynamical QuasiParticle Model (DQPM) [10] which describes QCD properties in terms of 'resummed' single-particle Green functions. In Ref. [11], the actual three DQPM parameters for the temperature-dependent effective coupling were fitted to the recent lattice QCD results of Ref. [12]. The latter lead to a critical temperature $T_c \approx 160$ MeV which corresponds to a critical energy density of $\epsilon_c \approx 0.5$ GeV/fm$^3$. In PHSD the parton spectral functions $\rho_j$ ($j = q, \bar{q}, g$) are no longer $\delta-$ functions in the invariant mass squared as in conventional cascade or transport models but depend on the parton mass and width parameters which were fixed by fitting the lattice QCD results from Ref. [12]. We recall that the DQPM allows one to extract a potential energy density $V_p$ from the space-like part of the energy-momentum tensor as a function of the scalar parton density $\rho_s$. Derivatives of $V_p$ w.r.t. $\rho_s$ then define a scalar mean-field potential $U_s(\rho_s)$ which enters into the equation of motion for the dynamical partonic quasiparticles. Furthermore, a two-body interaction strength can be extracted from the DQPM as well from the quasiparticle width in line with Ref. [13]. The transition from partonic to hadronic d.o.f. (and vice versa) is described by covariant transition rates for the fusion of quark-antiquark pairs or three quarks (antiquarks), respectively, obeying flavor current-conservation, color neutrality as well as energy-momentum conservation [9,11]. Since the dynamical quarks and antiquarks become very massive close to the phase transition, the formed resonant 'prehadronic' color-dipole states ($q\bar{q}$ or $qqq$) are of high invariant mass, too, and sequentially decay to the groundstate meson and baryon octets increasing the total entropy.

On the hadronic side PHSD includes explicitly the baryon octet and decouplet, the $0^-$- and $1^-$-meson nonets as well, as selected higher resonances as in the Hadron-String-Dynamics (HSD) approach [14,15]. Hadrons of higher masses ($> 1.5$ GeV in case of baryons and $> 1.3$ GeV for mesons) are treated as 'strings' (color-dipoles) that decay to the known (low-mass) hadrons, according to the JETSET algorithm [16]. Note that PHSD and HSD merge at low energy density, in particular below the critical energy density $\epsilon_c \approx 0.5$ GeV/fm$^3$. For more detailed descriptions of PHSD and its ingredients we refer the reader to Refs. [10,11,17,18].

The PHSD approach was applied to nucleus-nucleus collisions from $s_{NN}^{1/2} \sim 5$ to 200 GeV in Refs. [9,11] in order to explore the space-time regions of partonic matter. It was found that even central collisions at the top-SPS energy of $\sqrt{s_{NN}}$ =17.3 GeV show a large fraction of

nonpartonic, *i.e.* hadronic or string-like matter, which can be viewed as a hadronic corona. This finding implies that neither hadronic nor only partonic 'models' can be employed to extract physical conclusions in comparing model results with data.

## 3 Strangeness enhancement

As found in Ref. [9] the impact of the partonic degrees of freedom in PHSD on the longitudinal rapidity distribution of protons, pions and kaons is only small in central Pb+Pb collisions at SPS energies from 40 to 158 A·GeV. Additional experimental information is provided by the centrality dependence of the strange (and antistrange) baryon yield. In this respect we compare in Fig. 1 the multiplicities of $(\Lambda+\Sigma^0)/N_{wound}$ (l.h.s.) and $(\bar{\Lambda}+\bar{\Sigma}^0)/N_{wound}$ (r.h.s.) as a function of the number of wounded nucleons $N_{wound}$ for Pb+Pb collisions at 158 A·GeV at mid-rapidity from PHSD (blue solid lines) and HSD (red dashed-dotted lines) to the experimental data from the NA57 Collaboration [21] (open triangles) and the NA49 Collaboration [22] (solid dots). The (green) full squares correspond to the 10% central data points at midrapidity from Ref. [23]. We mention that we employ the same definition of wounded nucleons $N_{wound}$ as the NA49 Collaboration. Whereas the HSD and PHSD calculations both give a reasonable description of the $\Lambda + \Sigma^0$ yield of the NA49 Collaboration, both models underestimate the NA57 data (open triangles) by about 30%. An even larger discrepancy in the data from the NA49 and NA57 Collaborations is seen for $(\bar{\Lambda} + \bar{\Sigma}^0)/N_{wound}$ (r.h.s.); here the PHSD calculations give results which are in between the NA49 data (solid dots) and the NA57 data (open triangles). We also see that HSD underestimates the $(\bar{\Lambda} + \bar{\Sigma}^0)$ midrapidity yield at all centralities.

The latter results suggest that the partonic phase does not show up explicitly in an enhanced production of strangeness (or in particular strange mesons and baryons) but leads to a different redistribution of antistrange quarks between mesons and antibaryons in the hadronization process. To examine this issue in more detail we show in Fig. 1 (bottom part) the multiplicities of $\Xi^-$ baryons (l.h.s.) and $\bar{\Xi}^+$ antibaryons (r.h.s.) - devided by $N_{wound}$ - as a function of the number of wounded nucleons for Pb+Pb collisions at 158 A·GeV at mid-rapidity from PHSD and HSD in comparison to the experimental data from the NA57 Collaboration [21] and the NA49 Collaboration [23,22]. The situation is very similar to the case of the strange baryons and antibaryons before: we find no sizeable differences in the double strange baryons from HSD and PHSD – in a good agreement with the NA49 data – but observe a large enhancement in the double strange antibaryon yield for PHSD relative to HSD.

We note in passing that in Ref. [24] similar results have been obtained in the HSD approach by including multi-meson fusion channels in the production of baryon-antibaryon pairs. In the latter approach mesonic states have been propagated also at local energy density above critical energy density of $\varepsilon_C \simeq 0.5$ GeV/fm$^3$ and been allowed to interact. Such multi-meson fusion channels at high energy-density also lead to approximate chemical equilibrium. However, in PHSD mesonic reactions channels can not occur at energy densities above $\varepsilon_C$ since here partonic degrees-of-freedom play the dominant role. The interaction rate of multi-meson channels decreases drastically for $\varepsilon < \varepsilon_C$ due to the reduced hadron densities. Note that in Ref. [25] the high-energy density phase treated by hydro which implicitly implies thermal and chemical equilibrium. At least a chemical equilibration at high energy density appears mandatory to describe the experimental data. Such an equilibrium may be generated by partonic channels [9], by multi-hadronic interaction [24] or by model assumptions [25].

## 4 Results for dilepton spectra in comparison to experimental data

We directly continue with the results from PHSD in comparison with the available experimental data on dilepton production from SPS to RHIC energies. For details we refer the reader to Refs. [7,8,28].

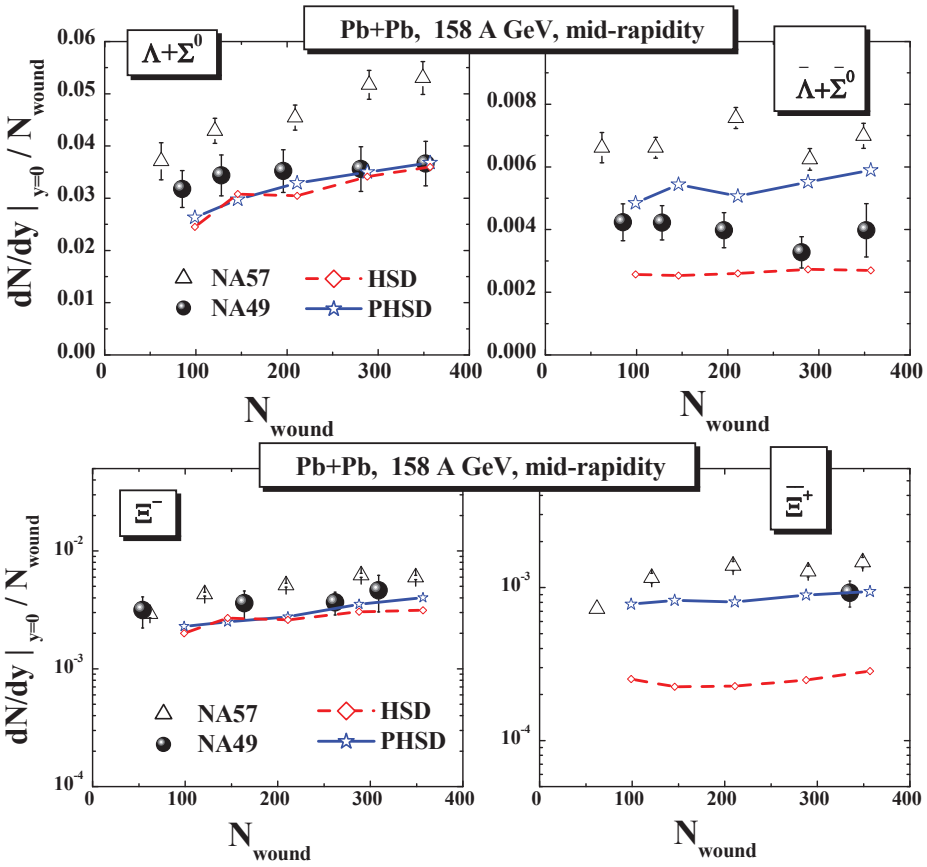


**Fig. 1. Top:** The multiplicities of $(\Lambda + \Sigma^0)/N_{wound}$ (l.h.s.) and $(\bar{\Lambda} + \bar{\Sigma}^0)/N_{wound}$ (r.h.s.) as a function of the number of wounded nucleons for Pb+Pb collisions at 158 A·GeV at mid-rapidity from PHSD (blue solid lines) and HSD (red dashed-dotted lines) in comparison to the experimental data from the NA57 Collaboration [21] (open triangles) and the NA49 Collaboration [22] (solid dots). The calculations have an error of 5−10% due to limited statistics. **Bottom:** The multiplicities of $\Xi^-/N_{wound}$ (l.h.s.) and $\bar{\Xi}^+/N_{wound}$ (r.h.s.) vs $N_{wound}$ for Pb+Pb collisions at 158 A·GeV at mid-rapidity. Line coding as above.

### 4.1 Dileptons at SPS energies

We start with a comparison of PHSD results to experimental data for dileptons from In+In collisions at 160 A GeV measured by the NA60 Collaboration. As has been shown in our early study [33] based on the off-shell HSD transport model without including an explicit partonic phase, the NA60 data favour a collisional broadening scenario for the in-medium modification of the vector mesons spectral function. However, the off-shell HSD calculations fail to explain the enhanced dilepton yield at large invariant masses $M > 1$GeV - cf. Fig. 2 of Ref. [33].

In Fig. 2 we present PHSD results for the dilepton excess over the known hadronic sources as produced in In+In reactions at 158 A GeV compared to the acceptance corrected data. We find here that the spectrum at invariant masses in the vicinity of the $\rho$ peak is well reproduced by the $\rho$ meson yield, if a broadening of the meson spectral function in the medium is assumed, while the partonic sources account for the yield at high masses. Our analysis shows that the contributions of the '$4\pi$' processes (shown by the lines with symbols) are very much supressed as was first noted by the authors of Ref. [3].

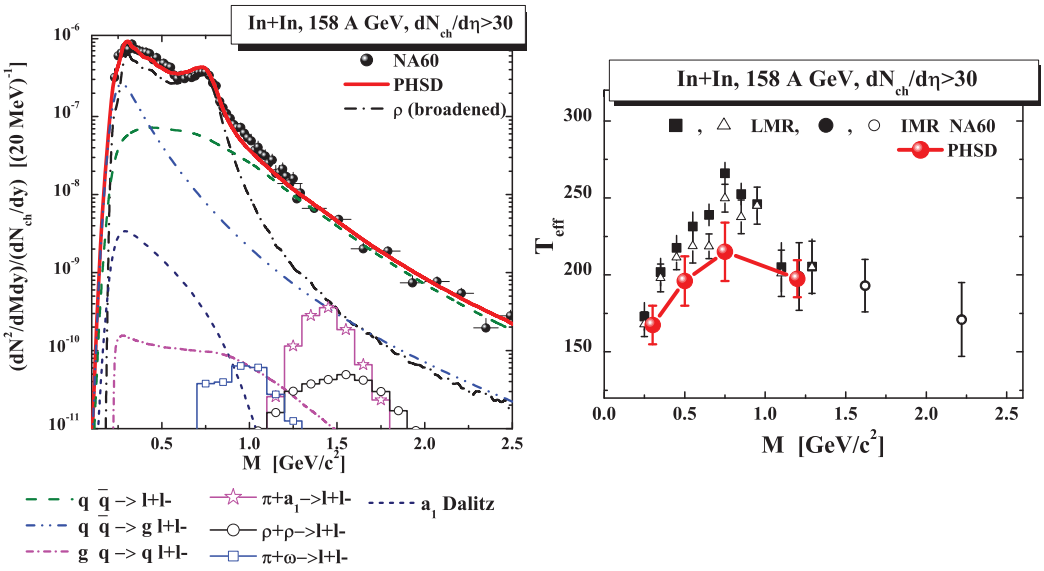


**Fig. 2.** Left: Acceptance corrected mass spectra of excess dimuons from In+In at 158 A GeV integrated over $p_T$ in $0.2 < p_T < 2.4$ GeV from PHSD compared to the data of NA60 [26]. The dash-dotted line shows the dilepton yield from the in-medium $\rho$ with a broadened spectral function, the dashed line presents the yield from the $q + \bar{q}$ annihilation, the dash-dot-dot line gives the contribution of the gluon Bremsstrahlung process ($q\bar{q} \to g l^+ l^-$), while the solid line is the sum of all contributions. For the description of the other lines, which correspond to the non-dominant channels, we refer to the figure legend. Right: The inverse slope parameter $T_{eff}$ of the dimuon yield from In+In at 158 A GeV as a function of the dimuon invariant mass in PHSD compared to the data of the NA60 Collaboration [26, 27].

One concludes from Fig. 2 that the measured spectrum for $M > 1$ GeV is dominated by the *partonic* sources. Indeed, the domination of the radiation from the QGP over the hadronic sources in PHSD is related to a rather long – of the order or 3 fm/c – evolution in the partonic phase (in co-existence with the space-time separated hadronic phase) on one hand (cf. Fig. 10 of Ref. [9]) and the rather high initial energy densities created in the collision on the other hand (cf. Fig. 6 of Ref. [28]). In addition, we find from Fig. 2 that in PHSD the partonic sources also have a considerable contribution to the dilepton yield for $M < 0.6$ GeV. The yield from the two-to-two process $q + \bar{q} \to g + l^+ l^-$ is especially important close to the threshold ($\approx 0.211$ GeV). This conclusion from the microscopic calculations is in qualitative agreement with the findings of an earlier (more schematic) investigation in Ref.[29] as well as the hybrid model calculations in Ref. [30] based on the hydro + UrQMD combined approach.

The comparison of the mass dependence of the slope parameter evolution in PHSD and the data is shown explicitly in right part of Fig. 2. Including partonic dilepton sources allows us to reproduce in PHSD the $m_T$-spectra as well as the finding of the NA60 Collaboration [26, 27] that the effective temperature of the dileptons (slope parameters) in the intermediate mass range is lower than that of the dileptons in the mass bin $0.6 < M < 1$ GeV, which is dominated by hadronic sources (cf. Fig. 2, right). The softening of the transverse mass spectrum with growing invariant mass implies that the partonic channels occur dominantly before the collective radial flow has developed. Also, the fact that the slope in the lowest mass bin and the highest one are approximately equal – both in the data and in PHSD – can be traced back to the two windows of the mass spectrum that in our picture are influenced by the radiation from the sQGP: $M = 2M_\mu - 0.6$ GeV and $M > 1$ GeV. For more details we refer the reader to Ref. [8].

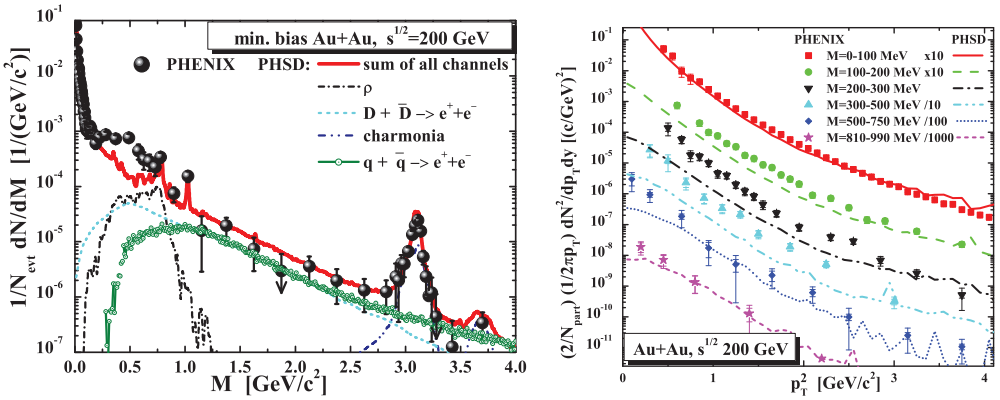


**Fig. 3.** Left: The PHSD results for the invariant mass spectra of inclusive dileptons in Au+Au collisions at $\sqrt{s_{NN}} = 200$ GeV within the PHENIX acceptance cuts in comparison to the data from the PHENIX Collaboration [31,32] The different lines indicate the contributions from different channels as specified in the figure. Right: The PHSD results for the transverse-momentum spectra of dileptons from minimum bias Au+Au collisions at $\sqrt{s_{NN}} = 200$ GeV in different mass bins compared to the data from the PHENIX Collaboration [31,32].

### 4.2 Dileptons at RHIC energies

Now we are coming to the top RHIC energy of $\sqrt{s_{NN}} = 200$ GeV and present the most important findings from the PHSD study in Ref. [7]. In the left part of Fig. 3 we show our results for the invariant mass spectra of inclusive dileptons in Au+Au collisions for the acceptance cuts on single electron transverse momenta $p_{eT}$, pseudorapidities $\eta_e$, azimutal angle $\phi_e$, and dilepton pair rapidity $y$: $p_{eT} > 0.2$ GeV, $|\eta_e| < 0.35$, $-3\pi/16 < \phi_e < 5\pi/16$, $11\pi/16 < \phi_e < 19\pi/16$, $|y| < 0.35$.

In the low mass region $M = 0 - 1.2$ GeV, the dilepton yield in the PHSD is dominated by hadronic sources and essentially coincides with the earlier HSD result [33]. Note that the collisional broadening scenario for the modification of the $\rho$-meson was used in the calculations presented in Fig. 3 that underestimates the PHENIX data from 0.2 to 0.7 GeV substantially. In contrast, the partonic radiation as well as the yield from correlated $D$-meson decays are dominant in the mass region $M = 1 - 3$ GeV as seen in Fig. 3 (left), i.e. in the mass region between the $\phi$ and $J/\Psi$ peaks. The dileptons generated by the quark-antiquark annihilation in the sQGP constitute about half of the observed yield in this intermediate-mass range. For $M > 2.5$ GeV the partonic yield even dominates over the D-meson contribution. Thus, the inclusion of the partonic radiation in the PHSD fills up the gap between the hadronic model results [33,34] and the data of the PHENIX Collaboration for $M > 1$ GeV, however, the early expectation of a partonic signal in the low mass dilepton spectrum is not verified by the microscopic PHSD calculations.

In order to investigate the momentum dependance of the "missing low mass yield", we have calculated the $p_T$-spectra of dileptons in different bins of invariant mass $M$. In the right part of Fig. 3 we show the measured transverse momentum spectra of dileptons for minimum bias Au+Au collisions at $\sqrt{s_{NN}} = 200$ GeV (symbols) in comparison with the spectra from the PHSD (lines) for six mass bins as indicated in the figure. Whereas the PHSD can well describe the dilepton spectra in the mass intervals [0,100 MeV] and [810 MeV, 990 MeV], it underestimates the low $p_T$ dileptons in the other mass bins, particularly in the mass bins [300 MeV, 500 MeV]. On the other hand, high $p_T$ dileptons are reproduced quite well by the PHSD calculations. We conclude that the missing dilepton yield for masses from 0.15 to 0.6 GeV is essentially due to a severe underestimation of the data at low $p_T$ by up to an order of magnitude. We recall that at top SPS energies the low $p_T$ dilepton yield could be attributed to $\pi\pi$ annihilation channels, i.e. to the soft hadronic reactions in the expansion phase of the

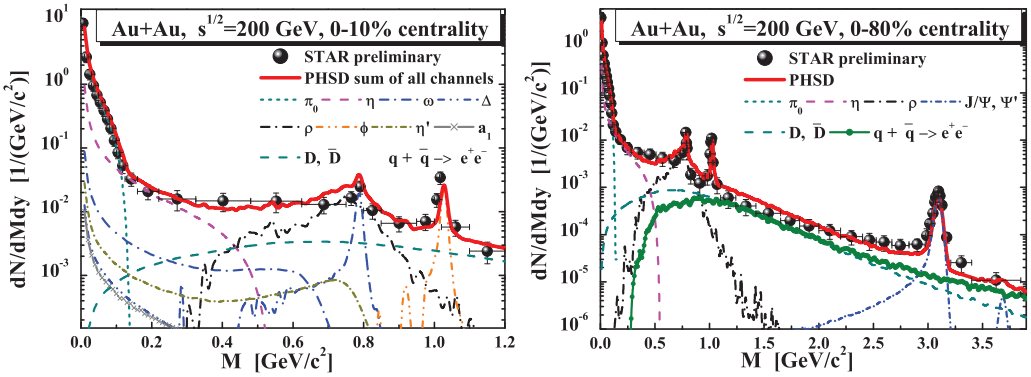


**Fig. 4.** The PHSD results for the invariant mass spectra of dileptons in Au+Au collisions at $\sqrt{s_{NN}}$ = 200 GeV for $M = 0-1.2$ GeV (left part) and for $M = 0-4$ GeV (right part) and 0 - 10 % centrality within the cuts of the STAR experiment. The preliminary data from the STAR Collaboration are adopted from Ref. [35].

system. These channels are, however, insufficient to describe the very low slope of the $p_T$ spectra at the top RHIC energy.

In order to shed some light on the 'PHENIX puzzle' we step to a comparison of the PHSD predictions with the preliminary STAR data measured for Au+Au collisions at $\sqrt{s_{NN}} = 200$ GeV with the acceptance cuts on single electron transverse momenta $p_{eT}$, single electron pseudorapidities $\eta_e$ and the dilepton pair rapidity $y$, i.e. $0.2 < p_{eT} < 5$ GeV, $|\eta_e| < 1$, $|y| < 1$. Our predictions for the dilepton yield within these cuts are shown in Fig. 4 for 0-80% centrality. One can observe generally a good agreement with the preliminary data from the STAR Collaboration [35] in the whole mass regime. Surprisingly, our calculations are also roughly in line with the low mass dilepton spectrum from STAR in case of central collisions whereas the PHSD results severely underestimate the PHENIX data. The observed yield from STAR can be accounted for by the known hadronic sources, i.e. the decays of the $\pi_0$, $\eta$, $\eta'$, $\omega$, $\rho$, $\phi$ and $a_1$ mesons, of the $\Delta$ particle and the semileptonic decays of the $D$ and $\bar{D}$ mesons, where the collisional broadening of the $\rho$ meson is taken into account.

The discrepancy between the PHENIX and STAR data will have to be investigated closer by the experimental collaborations. Furthermore, the upgrade of the PHENIX experiment with a hadron blind detector should provide decisive information on the origin of the low mass dileptons produced in the heavy-ion collisions at $\sqrt{s_{NN}} = 200$ GeV.

## 5 Conclusions

We close this contribution by noting that the measurement of hadronic resonances is a promising probe of the dynamical processes in heavy-ion collisions at all energy regimes. E.g., the enhancement of multi-strangene resonance production can signal the QGP formation. Futhermore, the low-mass dileptons provide information on the vector meson spectral function in the medium whereas the high mass part from 1.1 to 3 GeV can be attributed dominantly to the partonic annihilation in the QGP phase. At the higher RHIC energies the modifications of the low-mass sector are less pronounced than at SIS and SPS energies, however, the dilepton emissivity from the sQGP becomes substantial or even dominant relative to the background from $D$-meson decays at RHIC and LHC energies.

The author acknowledges the financial support within the "HIC for FAIR" framework of the "LOEWE" program. Furthermore, she likes to thank W. Cassing, C. M. Ko, V. Konchakovski, O. Linnyk, J. Manninen and V. Ozvenchuk for their contributions to the dilepton

and strangeness study presented in this contribution and C. Markert for stimulating discussions.

## References

1. M. M. Aggarwal *et al.*, STAR Colaboration, Phys. Rev. **C71** (2005) 064902; Phys. Rev. Lett. **97** (2006) 132301; arXiv:1006.1961.
2. E. V. Shuryak, Phys. Lett. **B78**, 150 (1978), Sov. J. Nucl. Phys. **28** (1978) 408, Yad. Fiz. **28** (1978) 796.
3. C. Song, C. M. Ko, and C. Gale, Phys. Rev. **D50** (1994) 1827.
4. G. Q. Li and C. Gale, Phys. Rev. C **58** (1998) 2914.
5. H. van Hees and R. Rapp, Phys. Rev. Lett. **97** (2006) 102301.
6. H. van Hees and R. Rapp, Nucl. Phys. A **806** (2008) 339.
7. O. Linnyk, W. Cassing, J. Manninen, E. L. Bratkovskaya and C. M. Ko, Phys. Rev. C **85**, 024910 (2012).
8. O. Linnyk, E. L. Bratkovskaya, V. Ozvenchuk, W. Cassing and C. M. Ko, Phys. Rev. C **84** (2011) 054917.
9. W. Cassing and E. L. Bratkovskaya, Nucl. Phys. **A831** (2009) 215.
10. W. Cassing, Nucl. Phys. A **A795** (2007) 70.
11. E. L. Bratkovskaya, W. Cassing, V. P. Konchakovski, and O. Linnyk, Nucl. Phys. **A856** (2011) 162.
12. Y. Aoki *et al.*, JHEP **0906** (2009) 088.
13. A. Peshier and W. Cassing, Phys. Rev. Lett. **94** (2005) 172301.
14. W. Ehehalt and W. Cassing, Nucl. Phys. **A 602** (1996) 449.
15. W. Cassing and E. L. Bratkovskaya, Phys. Rep. **308** (1999) 65.
16. H. U. Bengtsson and T. Sjöstrand, Comp. Phys. Commun. **46** (1987) 43.
17. W. Cassing, Nucl. Phys. **A 791** (2007) 365.
18. W. Cassing, Eur. J. Phys. **168** (2009) 3.
19. C. Alt *et al.*, NA49 Collaboration, Phys. Rev. **C66** (2002) 054902; Phys. Rev. C 77, 2008, P. 024903.
20. J. Geiss, W. Cassing and C. Greiner, Nucl. Phys. **A644** (1998) 107.
21. F. Antinori *et al.*, Phys. Lett. **B595** (2004) 68; J. Phys. G: Nucl. Phys. **32** (2006) 427.
22. T. Anticic *et al.*, NA49 Collaboration, Phys. Rev. C **80** (2009) 034906.
23. C. Alt *et al.*, NA49 Collaboration, Phys. Rev. **C78** (2008) 034918.
24. W. Cassing, Nucl. Phys. **A 700** (2002) 618.
25. H. Petersen *et al.*, Phys. Rev. C **80** (2009) 054910.
26. R. Arnaldi *et al.*, NA60 Collaboration, Eur. Phys. **C 59** (2009) 607.
27. R. Arnaldi *at al.*, NA60 Collaboration, Phys. Rev. Lett. **96** (2006) 162302; J. Seixas *et al.*, J. Phys. G **34** (2007) S1023; S. Damjanovic *et al.*, Nucl. Phys. **A 783** (2007) 327c; R. Arnaldi *et al.*, Eur. Phys. J **C61** (2009) 711.
28. O. Linnyk, E. L. Bratkovskaya, and W. Cassing, Int. J. Mod. Phys. **E17** (2008) 1367.
29. J. Alam, T. Hirano, J. K. Nayak, and B. Sinha, arXiv:0902.0446.
30. E. Santini et al., Phys. Rev. C **84** (2011) 014901.
31. A. Toia *et al.*, PHENIX Collaboration, Nucl. Phys. **A774** (2006) 743.
32. A. Adare *et al.*, PHENIX Collaboration, Phys. Rev. **C81** (2010) 034911.
33. E. L. Bratkovskaya, W. Cassing, and O. Linnyk, Phys. Lett. **B670** (2009) 428.
34. J. Manninen, E. L. Bratkovskaya, W. Cassing and O. Linnyk, Eur. Phys. J. C **71** (2011) 1615.
35. J. Zhao *et al.*, STAR Collaboration, arXiv:1106.6146[nucl-ex].